Decomposition Kinetics of Perfluorinated Sulfonic Acids

M. Yasir Khan[a], Sui So[a], Gabriel da Silva[a],*

[a]Department of Chemical Engineering, University of Melbourne, Victoria 3010, Australia.

*Corresponding author. Email: gdasilva@unimelb.edu.au

Abstract

Perfluorooctanesulfonic acid (PFOS) is a widespread and persistent pollutant of concern to human health and the environment. Although incineration is often used to treat material contaminated with PFOS and related per- and polyfluoroalkyl substances (PFAS), little is known about the precise chemical mechanism for the thermal decomposition of these substances of concern. Here, we present the first study of the thermal decomposition kinetics of PFOS and related perfluorinated acids, using computational chemistry and reaction rate theory methods. We discovered that preferred channel for PFOS decomposition is via an α-sultone that spontaneously decomposes to form perfluorooctanal and SO_2. At 1000 K the halflife for PFOS is predicted to be 0.2 s; decreasing sharply as temperature increases further. These results show that the acid headgroup in PFOS can be efficiently destroyed in incinerators operating at relatively modest temperatures. Understanding the exact decomposition mechanism and kinetics of PFOS will help to improve remediation technologies actively under development.

Keywords

Perfluorinated substances, Decomposition kinetics, Incineration, PFOS, PFOA, PFAS, Density functional theory, Transition state theory

INTRODUCTION

Perfluorooctanesulfonate (PFOS) and perfluorooctanoic acid (PFOA) are anthropogenic contaminants belonging to a large family of per- and polyfluoroalkyl substances (PFAS). These substances have been manufactured in large quantities mainly by electrochemical fluorination [1] and, due to their unique physicochemical properties, they had been used in a variety of consumer products and for a range of industrial applications [2]. The atmospheric, biologic, and aquatic degradation of some PFAS also produces PFOS [3–5] and other PFAS [6–8].

In the early 2000s, the primary American and European manufacturers ceased the production

of PFOS after it was globally detected in the human population, wildlife, soil and water [9]. The U.S. Environmental Protection Agency has established a health advisory level at 70 ng/L for the combined concentration of PFOS and PFOA in drinking water [10]. Human exposure to PFOS and PFOS-related products has been linked to cancer, kidney diseases, obesity, immune suppression, elevated cholesterol, and hormone disruption [11–13]. Because of the high energy of C–F bonds in PFAS, they resist physical, chemical, and biological degradation under standard atmospheric conditions, hence posing a persistent and bioaccumulative chronic threat to human health and wildlife. [14].

PFAS remediation methods can be classified into the following treatment groups: oxidative, reductive, and thermal [14–16]. Advanced Oxidation Processes (AOP) which utilize atomic oxygen, ozone, or hydroxyl radicals are viable solutions for the decomposition of recalcitrant organics. However, AOP have shown insufficient degradation efficiency for PFAS waste because highly electronegative fluorine atoms surround the carbon chain in these compounds. Furthermore, incomplete mineralisation identified in several AOP studies has indicated the formation of harmful intermediates [17]. To increase the degradation efficiency, conventional AOP are used in conjunction with at least one of the following reagents including Fenton's agent [17], sub- and supercritical water [18], zero-valent metal [19], and activated persulfate [20, 21]. Various reductive decomposition processes have been demonstrated to be useful for the defluorination of PFAS, including aqueous electrons, hydrated electrons, iron, alkaline 2-propanol, and UV-irradiated iodide, or - sulfites [22]. For example, ionising radiation via electron beams or gamma rays is promising for PFOS reduction [23]. Recently, sonochemical treatment of PFOS waste has reported complete mineralisation of fluorine [24].

While new PFAS degradation methods are still improving regarding operational cost and scalability [25], incineration and pyrolysis remain the most well-established destruction strategies for solid waste treatment. Incineration involves heating a waste to high temperatures with a typical residence time of several seconds. Laboratory scale analyses have shown PFOS to be more than 99% decomposed at 600 °C [14, 26]. In the incineration of PFOS and perfluorosulfonamides [26], Liquid Chromatography-Mass Spectrometry (LC/MS) measurements have not detected any traces

of PFOS in the reactor effluent implying that thermal treatment could be successfully used for the decomposition of these wastes. It was also demonstrated that perfluorosulfonamide incineration is not a potential source of PFOS to the environment and the presence of SO_2 in the exhaust stream suggests that this is the dominant sink for sulfur. Wang et al. [27] examined hydrated lime $(Ca(OH)_2)$ promoted incineration of PFOS sludge at low temperature (350 °C). The lime treatment of PFOS sludge between 350 °C to 900 °C releases fluorine (defluorination) which subsequently reacts to form CaF_2 and $Ca_5(PO_4)_3F$ phases along with the following gas fragments; $\cdot CF$, $\cdot CHF_2$, $\cdot CF_3$, and $\cdot C_3F_5$. It was also noted that between 600 to 900 °C, an increase in the retention time, temperature or both declines the gaseous CaF_2 content possibly due to the reaction with SiO_2, H_2O, and $Ca(OH)_2$ [28]. The mechanism of PFOS decomposition is fundamental to understand and improve thermal treatment methods.

Some product identification based experimental studies have been carried out, in an effort to elucidate the PFOS combustion mechanism [19, 26, 29, 30]. The terminal functional groups ($-SO_3H$, $-COOH$, $-SO_2NH_2$, etc.) have been observed to be mostly detached during PFAS incineration. For example, in a review article by Vecitis et al. a mechanism for PFOS pyrolysis was reported, where it was proposed that thermolysis begins with breaking of the C–S bond, leading to the formation of SO_3, HF, CF_2, and perfluoroalkene [29]. While CF_2, CF_3, C_2F_6, C_2F_4, SO_x and HF are the observed lighter end-products of PFOS pyrolysis, of which the carbonaceous products transform into CO_x in the presence of oxidizing media (water and/or air) [18, 26]. In the $Ca(OH)_2$ promoted thermal treatment of PFOS, Wang et al. [30] have demonstrated a slightly different mechanism for PFOS decomposition. A hydrodefluorination (conversion of C–F to C–H bonds) [31] mechanism is proposed that initiates with the elimination of fluorine which subsequently reacts with $Ca(OH)_2$ and forms CaF_2. The above mechanisms suggest different initiation pathways for decomposition of a potassium salt of PFOS; the former states direct C–S bond dissociation while the latter proposed fluorine elimination. Also, the reported mechanisms of PFOS decomposition have not included SO_2 which has been reported as the major sink of sulfur [7, 18, 26]. Analogous to PFOS, the combustion of PFOA also starts at the carboxylate terminal group; Krusic et al. [32] have suggested the elimination of HF and CO_2 at the α-position to produce perfluoroalkene as the initial

step for PFOA thermolysis.

The above experimental studies provide a broad overview of PFOS pyrolysis mechanisms, however, they provide limited information about the elementary decomposition pathways nor do they report kinetic parameters. Moreover, they fail to explain the formation of SO_2 in PFOS decomposition; SO_2 has been reported as the dominant sink for sulfur [7, 18, 26]. To develop and optimize thermal treatment technology for PFOS we must have a fundamental understanding of the elementary reaction mechanisms and kinetics. The present study provides the first detailed analysis of the thermal decomposition chemistry and kinetics of PFOS, using computational chemistry and statistical reaction rate theory techniques. This work identifies the likely products of the initial stages of PFOS decomposition and the rate at which these products will form as a function of temperature. Not only will this knowledge advance PFOS incineration techniques, but the understanding of the thermal behaviour of PFOS is also important for the development of advanced oxidation processes and other PFOS remediation methods because thermal treatment is one of the fundamental pre-treatment steps in most of them.

METHODS

Quantum chemistry calculations were carried out with the Gaussian 16 program suite [33]. The initial stage of work aimed to establish a reaction mechanism for PFOS using the model compounds perfluoromethanesulfonic acid (PFMS) and perfluoroethanesulfonic acid (PFES). These small model compounds allow us to identify computationally efficient theoretical model chemistries that are accurate for fluorinated sulfonic acids, in addition to establishing their mechanism. For the model compounds (PFMS, PFES), the geometries of reactants, products, intermediates, and transition states were optimized by employing different density functionals and basis sets (Supplementary Information). The equilibrium structures thus obtained were subsequently re-optimized a the M06-2X/6-31G(2df,p) level of theory and utilized in high-level composite G3X-K energy calculations [34]. For the full PFOS structure, the most accurate DFT calculations identified on the model compounds were applied. Intrinsic reaction coordinate (IRC) calculations have also been carried out to verify transition state connectivity. Rate coefficient calculations have been performed

using canonical transition state theory in the Multiwell-2016 collection of programs [35, 36]. All input parameters required for the rate coefficient calculations are provided in the Supplementary Information. The reaction rate coefficients and halflife are studied in the temperature range of 300–2000 K.

RESULTS AND DISCUSSION

PFMS Model Compound

The decomposition mechanism identified for PFMS on the basis of high-level G3X-K theory calculations is depicted in Fig. 1. The lowest energy direct bond-breaking reaction was found to be C–S cleavage, leading to the CF_3 and HSO_3 radicals. Terminal bond breaking has also been implicated in numerous experimental studies of long chain perfluorinated compounds [19, 26, 29]. This reaction does not proceed via a transition state (TS) and requires a barrier height of 72.8 kcal/mol. All other bond breaking reactions were found to be considerably higher in energy and are depicted in the Supplementary Information (Figure S2). Elimination of SO_3 via a H-shift reaction (TS2M) can also take place, forming HCF_3 (transition state structure shown in Fig. 3b). This is a known decomposition mechanism in sulfonic acids [15] and requires a barrier approximately equivalent to that for C–S bond cleavage. Slightly lower in energy than both of these conventional mechanisms is an isomerization process to yield the PFMS isomer $CF_3OS(O)OH$ (ISOPFMS, Fig. 3h). This reaction proceeds via TS3M, with barrier height of 68.4 kcal/mol. Although $CF_3OS(O)OH$ sits lower in energy than PFMS, it appears to be thermally unstable, with low-barrier decomposition channels available for SO_2 loss (TS5M and TS6M).

The lowest-energy decomposition mechanism for PFMS, by a considerable margin, involves HF elimination via TS1M (the transition state geometry represented in Fig. 3a). The energetic barrier here is calculated to be 45.3 kcal/mol, and this process will dominate the decomposition kinetics. Loss of HF leads to formation of the three-membered ring compound called difluoromethyl α-sultone (DFMS, Fig. 3g). Previously in the synthesis of γ-sultone [37], Morimoto et al. [38] have also suggested α-sultone as an unstable reaction intermediate. The potential surface energy
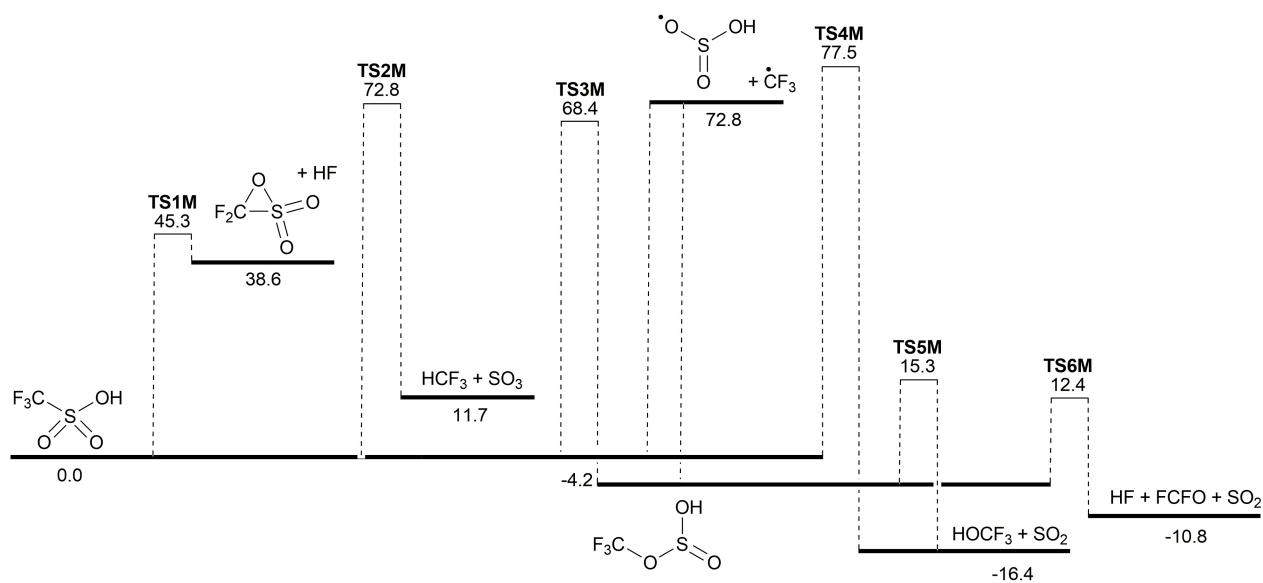
Figure 1: Thermal decomposition mechanism for PFMS. Energies are 0 K enthalpies in kcal/mol calculated at the G3X-K level of theory.

1 diagram shown in Fig. 2 also reveals that DFMS is a highly labile compound that spontaneously

2 decomposes to CF_2O and SO_2 with an almost negligible barrier of 5.4 kcal/mol. The elimination

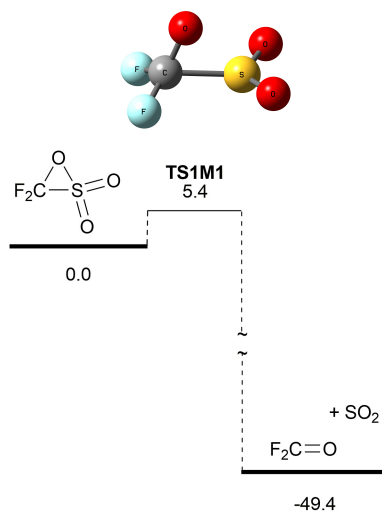3 of SO_2 takes place through transition state TS1MS1 (shown as an inset to Fig. 2).

Figure 2: Thermal decomposition of DFMS. Energies are 0 K enthalpies in kcal/mol calculated at the G3X-K level of theory.

4   The optimized geometries of PFMS, transition states and intermediates in the dissociation

5 process of PFMS are shown in Fig. 3. The lowest-energy decomposition of PFMS (Fig. 3a)

6 proceeds via a transition state resulting in the formation of DFMS. The major structural feature

of this transition state involves the elimination of HF and the creation of a new bond between the terminal oxygen and carbon. At the BMK/6-31++G(2df, p) level of theory, the C–S bond length and CSO bond angle are changed to 1.80 Å and 75.61° respectively in the transition state as compared to 1.87 Å and 107.19° in the ground state PFMS (Fig. 3i).

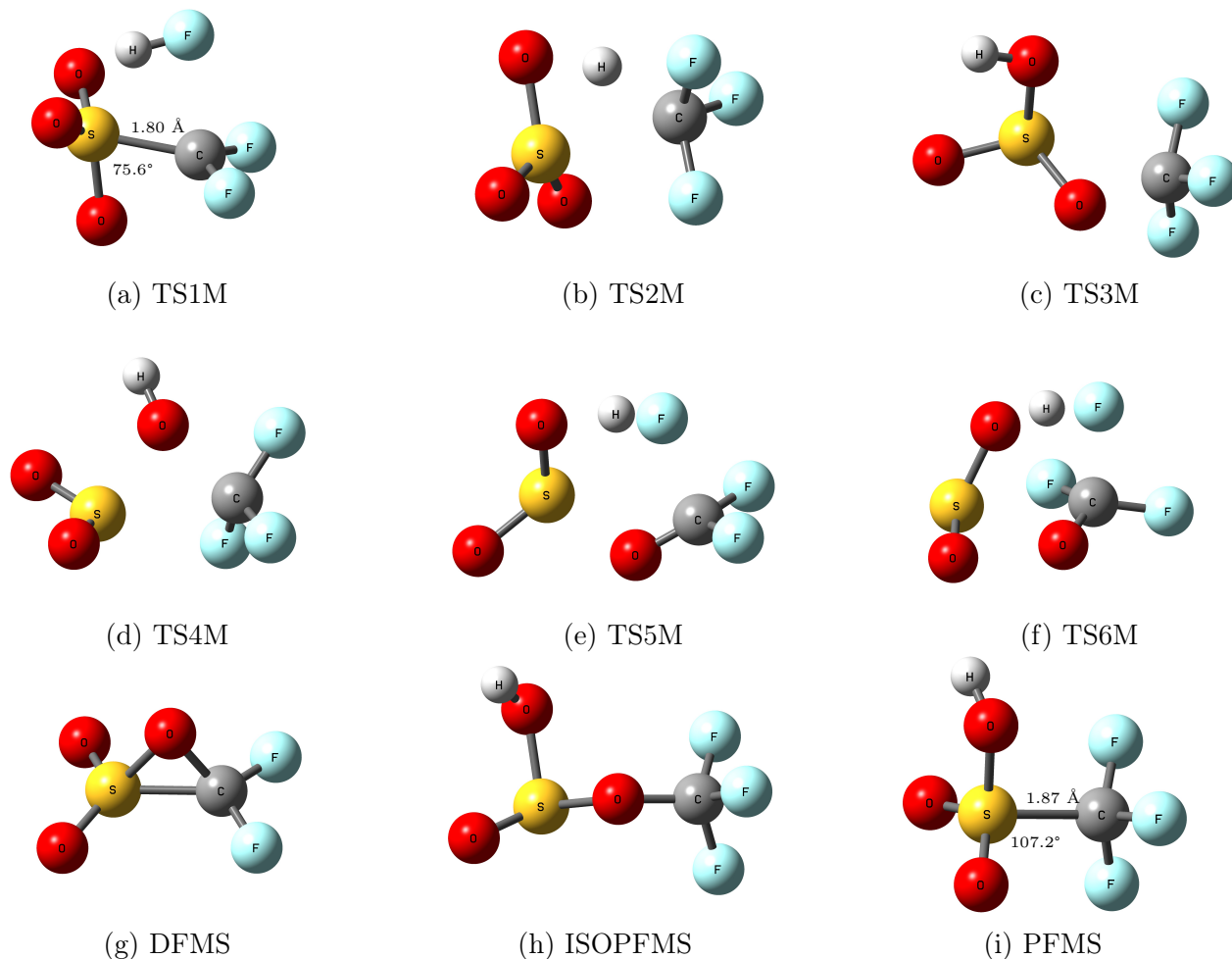| (a) TS1M | (b) TS2M | (c) TS3M |
| (d) TS4M | (e) TS5M | (f) TS6M |
| (g) DFMS | (h) ISOPFMS | (i) PFMS |

Figure 3: PFMS optimized transition state geometries (a-e) and ground state structure of (g) DFMS, (h) ISOPFMS, (f) PFMS at the BMK/6-31++G(2df,p) level of theory

Having established a decomposition mechanism for PFMS, attention turns to identifying model chemistries of reduced computational cost that can accurately reproduce the main features observed in this mechanism. Numerous density functional theory (DFT) methods were trialled in combination with different basis sets (Table S1 in the Supplementary Information). For all methods, the addition of diffuse basis functions dramatically improved accuracy for only a modest increase in computational cost. Extending basis set size from double-zeta to triple-zeta, on the other hand, resulted in only small improvements in accuracy for a significant extra cost. Accordingly, the aug-

mented double-zeta basis set 6-31++G(2df,p) was selected. Of the different DFT methods, the BMK and M06 functionals predicted the barrier height for HF elimination to similar precision, with BMK proving to be significantly more accurate for the other transition state energies. Accordingly, the BMK/6-31++G(2df,p) model chemistry [39] was adopted for the subsequent PFES and PFOS calculations.

PFES Model Compound

A mechanism illustrating the key features in the thermal decomposition of PFES is shown in Fig. 4. In this diagram, energies are included at the G3X-K and BMK/6-31++G(2df,p) levels of theory. The conventional sulfonic acid decomposition mechanisms leading to the HSO_3 radical and SO_3 proceed with similar energetics to their PFMS counterparts. The lowest-barrier decomposition reaction is still for HF elimination via TS1E to yield a tetrafluoroethyl α-sultone (TFES), although the G3X-K barrier height has increased from 45.3 to 55.8 kcal/mol. Note that the BMK model chemistry over-predicts this reaction barrier by almost 3 kcal/mol, in both the PFMS and PFES cases. Finally, a new HF elimination reaction is seen for PFES, leading to the products $CF_2=CF_2$ and SO_3 (TS3E). The transition state energy is slightly higher than for TS1E, although it is likely to be a competitive side-reaction in PFES decomposition. The optimized PFES and transition state geometries are displayed in Fig. 5.

Transition state theory has been used to calculate rate coefficients for PFES decomposition to the product sets $CF_3CFO + HF + SO_2$ and $CF_2CF_2 + HF + SO_3$, and to predict the PFES halflife as a function of temperature. An Arrhenius plot of the calculated rate coefficients is shown in Fig. 6, demonstrating that the acid head-group predominantly decomposes via initial elimination of HF, with subsequent dissociation to SO_2 and CF_3CFO is assumed to be instantaneous. The competing direct process of HF loss with CF_2CF_2 and SO_3 formation is a minor channel, even at very high temperatures.

Calculated halflife values for PFES are shown in the Supplementary Information Figure S3. Even at the relatively low incineration temperature of 800 K (527 °C) PFES is predicted to decompose rapidly, with a halflife of 2.4 seconds. At 1000 K the PFES halflife is only 2.5 ms. After
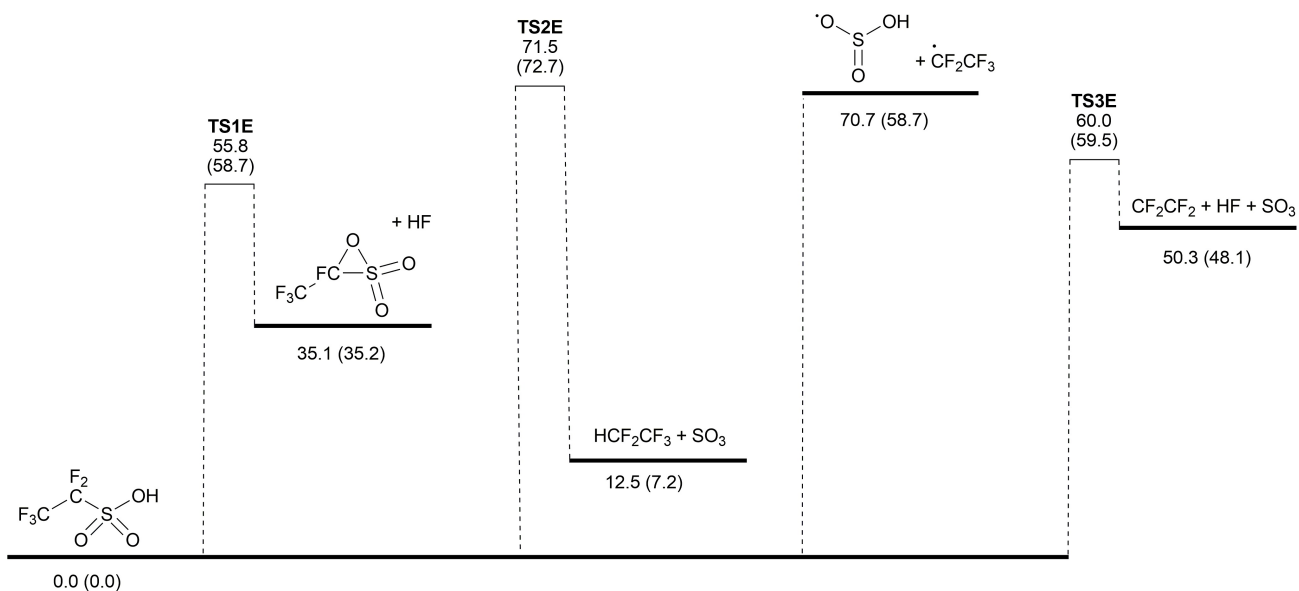
Figure 4: Simplified thermal decomposition mechanism for PFES. Energies are 0 K enthalpies in kcal/mol calculated at the G3X-K (BMK/6-31++G(2df,p)) levels of theory.

1 identifying two least resistive (TS1E, TS3E) routes for PFES decomposition, we next consider the

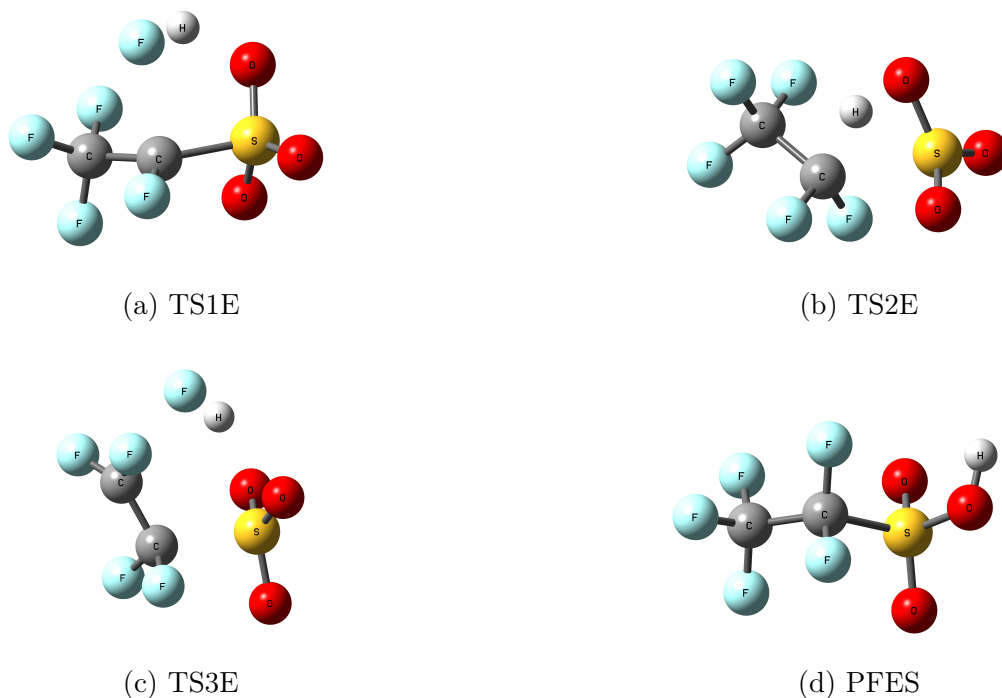2 thermolysis of the full PFOS molecule via these novel pathways.

(a) TS1E (b) TS2E (c) TS3E (d) PFES

Figure 5: PFES optimized transition state geometries (a-c) and ground state structure of PFES (d)

PFOS Decomposition

Following the preliminary calculations on the smaller PFMS and PFES model compounds, the BMK/6-31++G(2df,p) model chemistry was extended to PFOS itself for the two most important identified reaction channels. A potential energy surface is shown in Fig. 7 and the optimized geometries are represented in Fig. 8. Compared to PFES, the barrier (TSO1) for HF elimination to produce a PFOS derived α-sultone intermediate ($C_8F_{16}SO_3$) is very similar, at 57.5 kcal/mol (compared to 58.7 kcal/mol at the same level of theory, Fig. 4). In experimental study Song et al. (2013) have also reported that the photochemical decomposition of PFOA initiates with the elimination of fluorine atom at α-position of the terminal group [21]. As discussed, the BMK calculations are expected to somewhat over-predict this barrier height, and the calculated rate coefficients based on these energies may, therefore, be slight under-predictions. As with the model compounds, the α-sultone resulting from HF loss can readily dissociate with barrier height 8.5 kcal/mol to yield SO_2 and perfluorooctanal ($C_7F_{15}CFO$) via TSO12 transition state (Fig. 7b) The energies presented in Fig. 7b are calculated based on the α-sultone intermediate.
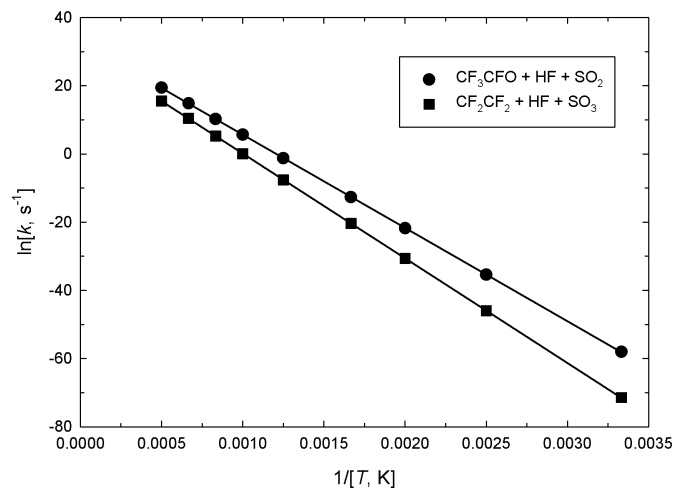
Figure 6: Arrhenius plot of calculated rate coefficients, k (s^{-1}), for thermal decomposition of PFES.

The competing decomposition channel for simultaneous HF and SO$_3$ loss was also considered, producing perfluorooct-1-ene (TSO2). The barrier height here was calculated to be 63.5 kcal/mol, considerably higher than that of TSO1. The formation of perfluoroolefin has also documented in the pyrolysis mechanism of PFOS which is based on an experimental study [29]. Further, the previous studies suggest that the decomposition proceeding from perfluorooctene-1 follows the chain shortening pathway and leads to the formation of CF$_2$, CF$_3$, C$_2$F$_6$, C$_2$F$_4$ and HF, among these the carbonaceous compounds transform into CO$_x$ in the presence of oxidizing media (water and/or air) [40–43].
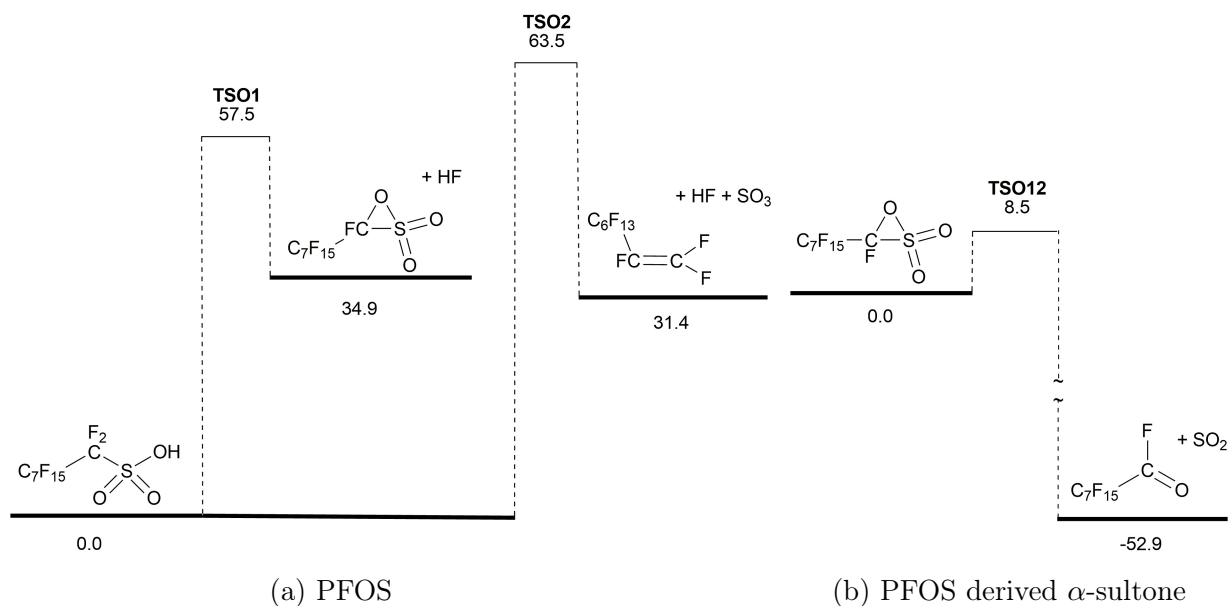
Figure 7: Thermal decomposition mechanism for PFOS and PFOS derived α-sultone intermediate. Energies are 0 K enthalpies in kcal/mol calculated at the BMK/6-31++G(2df,p) level of theory

The potential energy surface outlined in Fig. 7 was used to calculate rate coefficients for PFOS decomposition, according to transition state theory. Calculated rate coefficients and halflife for the two pathways considered are shown in Fig. 9 and Fig. 10 respectively at temperatures between 300 and 2000 K. Across all temperatures, HF loss to form SO_2 and the perfluorinated aldehyde is the dominant reaction channel. Rate coefficients for this reaction can be accurately reproduced using the Arrhenius parameters $A = 2.18 \times 10^{13}$ s^{-1} and $E_a = 58.4$ kcal/mol. As we can see from Fig. 10 that the PFOS halflife drops to below 1 s at 1000 K , which is again a relatively modest incineration temperature.
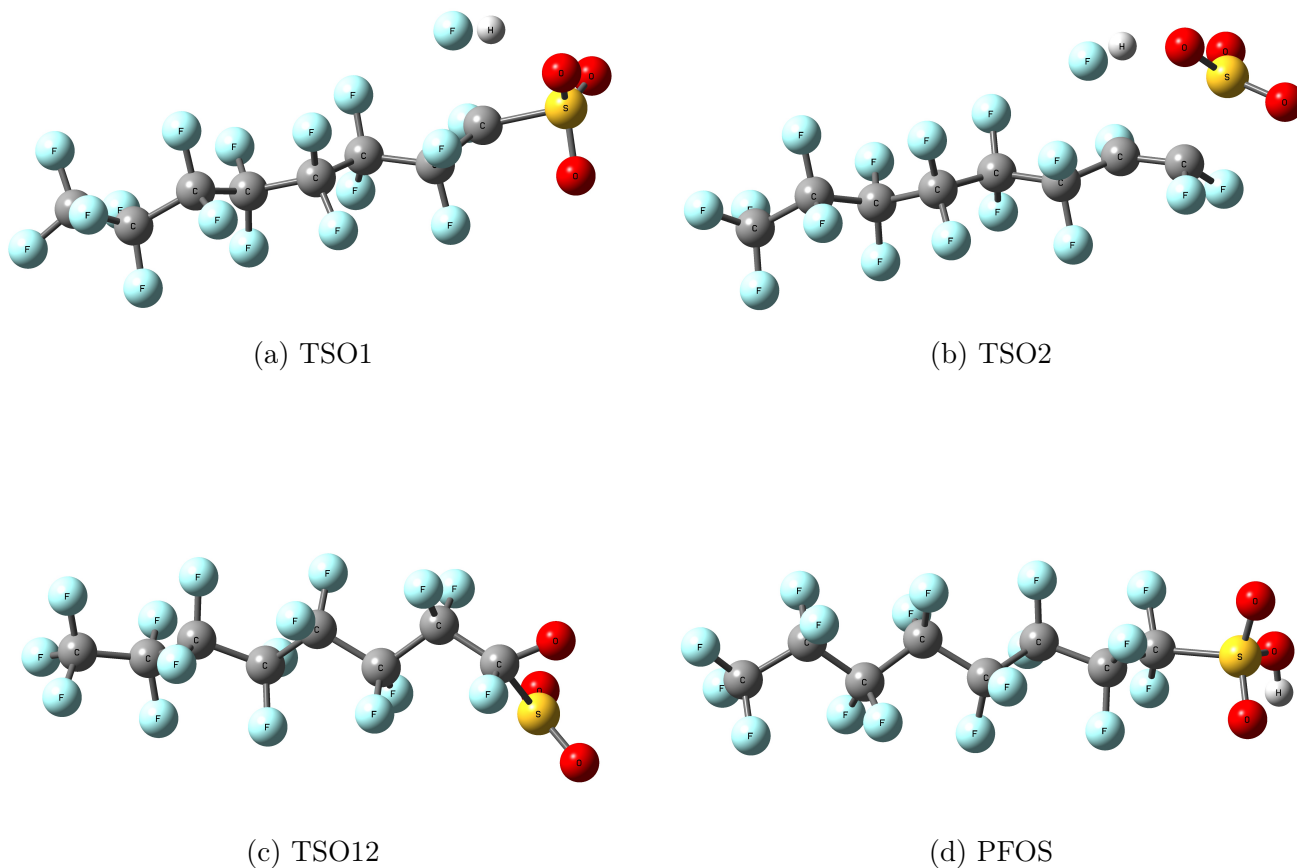
12

(a) TSO1

(b) TSO2

(c) TSO12

(d) PFOS

Figure 8: PFOS optimized transition state geometries (a-c) and ground state structure of PFOS (d)
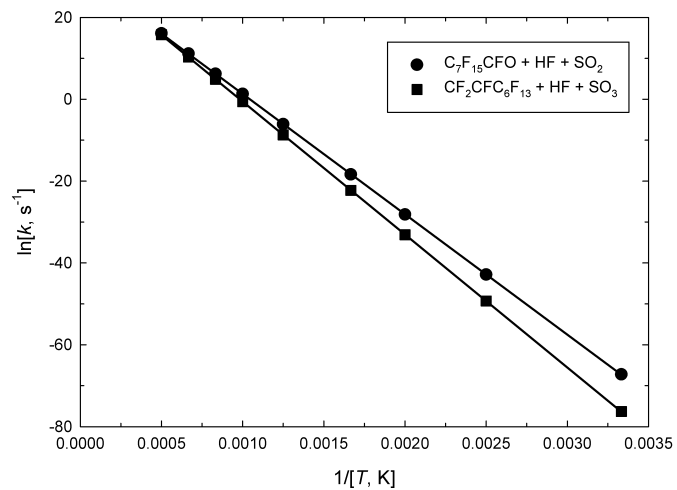

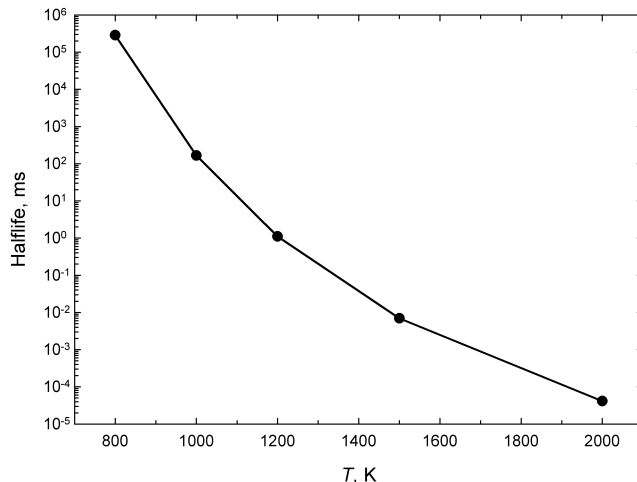Figure 9: Arrhenius plot of calculated rate coefficients, k (s^{-1}), for thermal decomposition of PFOS.

Figure 10: Calculated halflife (ms) for thermal decomposition of PFES.

This work suggests that perfluorooctanal will be the dominant initial fluorinated product of PFOS incineration, and the fate of fluorinated aldehydes in these systems therefore also needs to be considered. These compounds are known to be rapidly hydrolyzed to perfluorocarboxylic acids [29, 44], which is likely to be an important fate in the presence of water. Perfluorocarboxylic acids are chemical of concern in their own right, although laboratory scale studies on their incineration have demonstrated that they are up to 99 % decomposed in incinerators operating at 300 °C – 350 °C [32, 45]. Further work is required, however, to identify the ways in which oxygenated PFAS compounds break down during pyrolysis.

In summary, this work has identified that PFOS will undergo relatively rapid thermal decomposition, via a novel chemical mechanism. Moreover, our thermolysis mechanism explains the formation of SO_2 which has been detected in PFOS incineration effluent. We have also shown that SO_3 cannot only be produced via direct C–S bond dissociation but could also be formed via unimolecular elimination (transition state TSO2). We believe that the results of the present study not only provides a theoretical background for the PFOS thermal decomposition but would also help to: i) improve the current incineration technology by providing better-operating conditions; and ii) assist in the set up of new treatment facilities.

14

CONCLUSION

The thermal decomposition kinetics of PFOS and model compounds (PFMS and PFES) have been theoretically investigated by employing DFT and transition state theory. The C–S bond cleavage has been found to be the lowest energy direct bond-breaking reaction. However, the lowest-barrier decomposition for the model compounds and PFOS is HF elimination to yield α-sultone intermediate. Our findings demonstrate the α-sultone is an unstable compound that spontaneously releases SO_2. In addition, HF could also be eliminated leading to the formation of perfluoro-1-ene and SO_3, and this step could be the competitive reaction channels in thermolysis processes. Calculated rate coefficients and halflifes confirm that HF loss to form SO_2 and a perfluorinated aldehyde is the dominant reaction pathway at all temperatures. In summary, this study provides a better understanding of PFOS decomposition kinetics that will be used as a guide for improving and developing both current and new PFOS treatment facilities.

Conflicts of interest

The authors report no conflict of interest.

Acknowledgements

Bibliography

[1] Melissa M Schultz, Douglas F Barofsky, and Jennifer A Field. Fluorinated alkyl surfactants. *Environmental Engineering Science*, 20(5):487–501, 2003.

[2] Konstantinos Prevedouros, Ian T Cousins, Robert C Buck, and Stephen H Korzeniowski. Sources, fate and transport of perfluorocarboxylates. *Environmental science & technology*, 40 (1):32–44, 2006.

[3] Cora J Young, Vasile I Furdui, James Franklin, Roy M Koerner, Derek CG Muir, and Scott A Mabury. Perfluorinated acids in arctic snow: new evidence for atmospheric formation. *Environmental science & technology*, 41(10):3455–3461, 2007.

[4] Jessica C D'eon, Michael D Hurley, Timothy J Wallington, and Scott A Mabury. Atmospheric chemistry of N-methyl perfluorobutane sulfonamidoethanol, $C_4F_9SO_2N(CH_3)CH_2CH_2OH$: Kinetics and mechanism of reaction with OH. *Environmental science & technology*, 40(6):1862–1868, 2006.

[5] Gregg T Tomy, Sheryl A Tittlemier, Vince P Palace, Wes R Budakowski, Eric Braekevelt, Lyndon Brinkworth, and Ken Friesen. Biotransformation of N-ethyl perfluorooctanesulfonamide by rainbow trout (onchorhynchus mykiss) liver microsomes. *Environmental science & technology*, 38(3):758–762, 2004.

[6] Derek A Jackson, Timothy J Wallington, and Scott A Mabury. Atmospheric oxidation of polyfluorinated amides: historical source of perfluorinated carboxylic acids to the environment. *Environmental science & technology*, 47(9):4317–4324, 2013.

[7] Jonathan W Martin, David A Ellis, Scott A Mabury, MD Hurley, and TJ Wallington. Atmospheric chemistry of perfluoroalkanesulfonamides: kinetic and product studies of the OH radical and Cl atom initiated oxidation of N-ethyl perfluorobutanesulfonamide. *Environmental science & technology*, 40(3):864–872, 2006.

[8] David A Ellis, Jonathan W Martin, Amila O De Silva, Scott A Mabury, Michael D Hurley, Mads P Sulbaek Andersen, and Timothy J Wallington. Degradation of fluorotelomer alcohols: a likely atmospheric source of perfluorinated carboxylic acids. *Environmental science & technology*, 38(12):3316–3321, 2004.

[9] 3M Company. Environmental and health assessment of perfluorooctane sulfonic acid and its salts. Technical Report Docket AR-226-1486, US Environmental Protection Agency, 2003.

[10] Zachary R Hopkins, Mei Sun, Jamie C DeWitt, and Detlef RU Knappe. Recently detected drinking water contaminants: Genx and other per-and polyfluoroalkyl ether acids. *Journal-American Water Works Association*, 110(7):13–28, 2018.

[11] A Mahfouz J Morrissey Donohue and T M Duke. Health effects support document for perfluorooocatane sulfonate (PFOS). Technical Report 822-R-16-002, US Environmental Protection Agency, 2016.

[12] John W Stanifer, Heather M Stapleton, Tomokazu Souma, Ashley Wittmer, Xinlu Zhao, and L Ebony Boulware. Perfluorinated chemicals as emerging environmental threats to kidney health: A scoping review. *Clinical Journal of the American Society of Nephrology*, 13(10): 1479–1492, 2018.

[13] Geary W Olsen, Timothy R Church, John P Miller, Jean M Burris, Kristen J Hansen, James K Lundberg, John B Armitage, Ross M Herron, Zahra Medhdizadehkashi, John B Nobiletti, et al. Perfluorooctanesulfonate and other fluorochemicals in the serum of american red cross adult blood donors. *Environmental Health Perspectives*, 111(16):1892, 2003.

[14] Katarzyna H Kucharzyk, Ramona Darlington, Mark Benotti, Rula Deeb, and Elisabeth Haw-

ley. Novel treatment technologies for PFAS compounds: A critical review. *Journal of environmental management*, 204:757–764, 2017.

[15] Marek Trojanowicz, Anna Bojanowska-Czajka, Iwona Bartosiewicz, and Krzysztof Kulisa. Advanced oxidation/reduction processes treatment for aqueous perfluorooctanoate (PFOA) and perfluorooctanesulfonate (PFOS)–a review of recent advances. *Chemical Engineering Journal*, 336:170–199, 2018.

[16] Victor Andres Arias Espana, Megharaj Mallavarapu, and Ravi Naidu. Treatment technologies for aqueous perfluorooctanesulfonate (PFOS) and perfluorooctanoate (PFOA): A critical review with an emphasis on field testing. *Environmental Technology & Innovation*, 4:168–181, 2015.

[17] Horst Fr Schröder and Roland JW Meesters. Stability of fluorinated surfactants in advanced oxidation processes—a follow up of degradation products using flow injection–mass spectrometry, liquid chromatography–mass spectrometry and liquid chromatography–multiple stage mass spectrometry. *Journal of Chromatography A*, 1082(1):110–119, 2005.

[18] Hisao Hori, Yumiko Nagaoka, Taizo Sano, and Shuzo Kutsuna. Iron-induced decomposition of perfluorohexanesulfonate in sub-and supercritical water. *Chemosphere*, 70(5):800–806, 2008.

[19] Hisao Hori, Yumiko Nagaoka, Ari Yamamoto, Taizo Sano, Nobuyoshi Yamashita, Sachi Taniyasu, Shuzo Kutsuna, Issey Osaka, and Ryuichi Arakawa. Efficient decomposition of environmentally persistent perfluorooctanesulfonate and related fluorochemicals using zerovalent iron in subcritical water. *Environmental science & technology*, 40(3):1049–1054, 2006.

[20] BB Wang, MH Cao, ZJ Tan, LL Wang, SH Yuan, and J Chen. Photochemical decomposition of perfluorodecanoic acid in aqueous solution with VUV light irradiation. *Journal of hazardous materials*, 181(1-3):187–192, 2010.

[21] Zhou Song, Heqing Tang, Nan Wang, and Lihua Zhu. Reductive defluorination of perfluorooctanoic acid by hydrated electrons in a sulfite-mediated UV photochemical system. *Journal of hazardous materials*, 262:332–338, 2013.

[22] Ian Ross, Jeffrey McDonough, Jonathan Miles, Peter Storch, Parvathy Thelakkat Kochunarayanan, Erica Kalve, Jake Hurst, Soumitri S. Dasgupta, and Jeff Burdick. A review of emerging technologies for remediation of pfass. *Remediation Journal*, 28(2):101–126, 2018.

[23] Tae-Hun Kim, Seungho Yu, Yeowool Choi, Tae-Yong Jeong, and Sang Don Kim. Profiling the decomposition products of perfluorooctane sulfonate (PFOS) irradiated using an electron beam. *Science of The Total Environment*, 631:1295–1303, 2018.

[24] Vitthal L Gole, Asher Fishgold, Reyes Sierra-Alvarez, Pierre Deymier, and Manish Keswani. Treatment of perfluorooctane sulfonic acid (PFOS) using a large-scale sonochemical reactor. *Separation and Purification Technology*, 194:104–110, 2018.

[25] Lucia Rodriguez-Freire, Rajesh Balachandran, Reyes Sierra-Alvarez, and Manish Keswani. Effect of sound frequency and initial concentration on the sonochemical degradation of perfluorooctane sulfonate (PFOS). *Journal of hazardous materials*, 300:662–669, 2015.

[26] Office of Pollution Prevention & Toxics. Laboratory-scale thermal degradation of perfluorooctanyl sulfonate and related substances. Technical Report Docket AR226-1366, US Environmental Protection Agency, 2003.

[27] Fei Wang, Xingwen Lu, Kaimin Shih, and Chengshuai Liu. Influence of calcium hydroxide on the fate of perfluorooctanesulfonate under thermal conditions. *Journal of hazardous materials*, 192(3):1067–1071, 2011.

[28] Fei Wang, Kaimin Shih, Xingwen Lu, and Chengshuai Liu. Mineralization behavior of fluorine in perfluorooctanesulfonate (PFOS) during thermal treatment of lime-conditioned sludge. *Environmental science & technology*, 47(6):2621–2627, 2013.

[29] Chad D Vecitis, Hyunwoong Park, Jie Cheng, Brian T Mader, and Michael R Hoffmann. Treatment technologies for aqueous perfluorooctanesulfonate (PFOS) and perfluorooctanoate (PFOA). *Frontiers of Environmental Science & Engineering in China*, 3(2):129–151, 2009.

[30] Fei Wang, Xingwen Lu, Xiao-yan Li, and Kaimin Shih. Effectiveness and mechanisms of

defluorination of perfluorinated alkyl substances by calcium compounds during waste thermal treatment. *Environmental science & technology*, 49(9):5672–5680, 2015.

[31] Christos Douvris and Oleg V Ozerov. Hydrodefluorination of perfluoroalkyl groups using silylium-carborane catalysts. *Science*, 321(5893):1188–1190, 2008.

[32] Paul J Krusic, Alexander A Marchione, and D Christopher Roe. Gas-phase NMR studies of the thermolysis of perfluorooctanoic acid. *Journal of fluorine chemistry*, 126(11-12):1510–1516, 2005.

[33] MJ Frisch, GW Trucks, HB Schlegel, GE Scuseria, MA Robb, JR Cheeseman, G Scalmani, V Barone, B Mennucci, GA Petersson, et al. Gaussian 09, revision b. 01, gaussian. *Inc., Wallingford, CT*, 6492, 2010.

[34] Gabriel da Silva. G3X-K theory: A composite theoretical method for thermochemical kinetics. *Chemical Physics Letters*, 558:109–113, 2013.

[35] John R Barker, T. L Nguyen, J. F Stanton, C Aieta, M Ceotto, F Gabas, T. J. D Kumar, C. G. L Li, L. L Lohr, A Maranzana, N. F Ortiz, J. M Preses, J. M Simmie, J. A Sonk, and P. J Stimac. Multiwell-2016 software suite. `http://clasp-research.engin.umich.edu/multiwell/`, 2016.

[36] John R Barker. Multiple-well, multiple-path unimolecular reaction systems. i. multiwell computer program suite. *International Journal of Chemical Kinetics*, 33(4):232–245, 2001.

[37] Shovan Mondal. Recent developments in the synthesis and application of sultones. *Chemical reviews*, 112(10):5339–5355, 2012.

[38] Yoshiki Morimoto, Hajime Kurihara, and Takamasa Kinoshita. Can α-sultone exist as a chemical species? first experimental implication for intermediacy of α-sultone. *Chemical Communications*, (3):189–190, 2000.

[39] A Daniel Boese and Jan ML Martin. Development of density functionals for thermochemical kinetics. *The Journal of chemical physics*, 121(8):3405–3416, 2004.

[40] DR Burgess Jr, Michael Russel Zachariah, Wing Tsang, and Phillip Ray Westmoreland. Thermochemical and chemical kinetic data for fluorinated hydrocarbons. *Progress in Energy and Combustion Science*, 21(6):453–529, 1995.

[41] Gregory T Linteris, Valeri I Babushok, Peter B Sunderland, Fumi Takahashi, Viswanath R Katta, and Oliver Meier. Unwanted combustion enhancement by $C_6F_{12}O$ fire suppressant. *Proceedings of the Combustion Institute*, 34(2):2683–2690, 2013.

[42] CJ Cobos, K Hintzer, L Sölter, E Tellbach, A Thaler, and J Troe. Shock wave studies of the pyrolysis of fluorocarbon oxygenates. i. the thermal dissociation of C_3F_6O and CF_3COF. *Physical Chemistry Chemical Physics*, 19(4):3151–3158, 2017.

[43] Gary K Jarvis, Chris A Mayhew, and Richard P Tuckett. Study of the gas phase reactions of several perfluorocarbons with positive ions of atmospheric interest. *The Journal of Physical Chemistry*, 100(43):17166–17174, 1996.

[44] Shuzo Kutsuna and Hisao Hori. Rate constants for aqueous-phase reactions of SO_4^- with $C_2F_5C(O)O^-$ and $C_3F_7C(O)O^-$ at 298 K. *International Journal of Chemical Kinetics*, 39(5): 276–288, 2007.

[45] Paul J Krusic and D Christopher Roe. Gas-phase NMR technique for studying the thermolysis of materials: thermal decomposition of ammonium perfluorooctanoate. *Analytical chemistry*, 76(13):3800–3803, 2004.